Flight Dynamics of Aeroelastic Vehicles

Martin R. Waszak* and David K. Schmidt†
Purdue University, West Lafayette, Indiana

The nonlinear equations of motion for an elastic airplane are developed from first principles. Lagrange's equation and the Principle of Virtual Work are used to generate the equations of motion, and aerodynamic strip theory is then employed to obtain closed-form integral expressions for the generalized forces. The inertial coupling is minimized by appropriate choice of the body-reference axes and by making use of free vibration modes of the body. The mean axes conditions are discussed, a form that is useful for direct application is developed, and the rigid-body degrees of freedom governed by these equations are defined relative to this body-reference axis. In addition, particular attention is paid to the simplifying assumptions used during the development of the equations of motion. Since closed-form, analytic expressions are obtained for the generalized aerodynamic forces, insight can be gained into the effects of parameter variations that is not easily obtained from numerical models. An example is also presented in which the modeling method is applied to a generic elastic aircraft, and the model is used to parametrically address the effects of flexibility. The importance of residualizing elastic modes in forming an equivalent rigid model is illustrated, but as vehicle flexibility is increased, even modal residualization is shown to yield a poor model.

Introduction

WHEN a vehicle's structure exhibits sufficient rigidity, or stiffness, wide frequency separation results between those natural modes of the vehicle dominated by the rigid-body degrees of freedom and the remaining modes dominated by the elastic degrees of freedom. As a result, vehicle dynamic modeling, analysis, and synthesis activities frequently address either the rigid-body dynamics or the structural dynamics, but not both. Such a decoupling, however, is not always justified. Furthermore, modeling assumptions that imply decoupling, whether it truly exists or not, must be used with caution.

For example, in the development of a "flight mechanics model" for application to performance or stability and control analysis, handling qualities investigations, or flight control synthesis, a rigid-body assumption is frequently made. Elastic degrees of freedom are therefore absent from such a model from the outset. An example of the effect of such an assumption on a generic forward-swept-wing aircraft is presented in Ref. 1. Likewise, in the development of a "structural dynamic model" for flutter analysis, some or all of the rigid-body degrees of freedom are frequently not included.[2]

With structural weight always being minimized, with new materials (e.g., composites) being introduced, and with advanced, perhaps statically unstable vehicles employing high-authority feedback control systems, aeroelastic effects will become even more significant, and the frequency separation between the "rigid-body" modes and "elastic" modes will be reduced.

It would seem that an integrated, flexible vehicle model should be developed initially, then simplified appropriately after assembly, depending on the application. This, however, does not appear to be common practice, and techniques for doing so are not widely available in the archival literature or textbooks. In fact, Schwanz et al.[3] cite ten specific examples of problems occurring during flight tests of modern fighter aircraft. In each case the cause of the problem could be characterized as inadequate modeling or other inappropriate treatment of the aeroelastic effects on the vehicle dynamics and/or the flight control design.

In this paper, an integrated model will be assembled, with particular attention paid to the assumptions made at the various stages of the modeling. The intent in the development is to model large-amplitude displacements of the rigid-body degrees of freedom, leading to nonlinear equations of motion governing these degrees of freedom, expressed in terms of body-reference axes, rather than inertial axes. This allows the model to be used, for example, in real-time man-in-the-loop simulations. None of the techniques used in the development of the model are claimed to be new. The intent is to summarize the complete modeling process, if for no other reason than to encourage a more integrated modeling perspective.

The structural deformation is assumed sufficiently small, such that linear elastic theory is valid (Assumption 1). A set of normal vibration modes (frequencies and mode shapes) are assumed to be available, from a finite-element analysis, for example (Assumption 2). Application of Lagrange's equations then leads directly to the scalar, ordinary differential equations of motion, expressed in terms of the generalized forces associated with the aerodynamic and propulsive forces. The elastic and rigid-body degrees of freedom are ultimately coupled via these forces.

Closed-form integral expressions for the generalized aerodynamic forces are derived in terms of the in vacuo vibration mode shapes and an implicit aerodynamic force and moment distribution. Using simple aerodynamic strip theory,[4] analytical expressions are then obtained for the force and moment distributions, expressed in terms of the elastic and rigid-body degrees of freedom.

The use of strip theory here does not imply that this is the recommended technique for estimating the final numerical values for the generalized force coefficients. Some of the coefficients may be obtained, for example, from wind-tunnel tests on a rigid model, while others may be estimated via numerical techniques. Consequently, as improved estimates for the coefficients become available, they may be incorporated directly into the model, including unsteady aerodynamic coefficients.

However, the use of strip theory has two advantages. First, in the absence of any information, it provides a modeling approach early in the design cycle, and can lead to good results especially for high aspect ratios. Second, and more importantly, it leads to *analytical expressions*, which are more useful for providing insight into the model than arrays of numbers from a computer code, for example. Also, if accurate estimates of the coefficients are available for an existing vehicle configu-

Presented as Paper 86-2077 at the AIAA Atmospheric Flight Mechanics Conference, Williamsburg, VA, Aug. 18–20, 1986; received Jan. 9, 1987; revision received July 13, 1987.

*Graduate Research Assistant, School of Aeronautics and Astronautics. Student Member AIAA.

†Professor, School of Aeronautics and Astronautics. Associate Fellow AIAA.

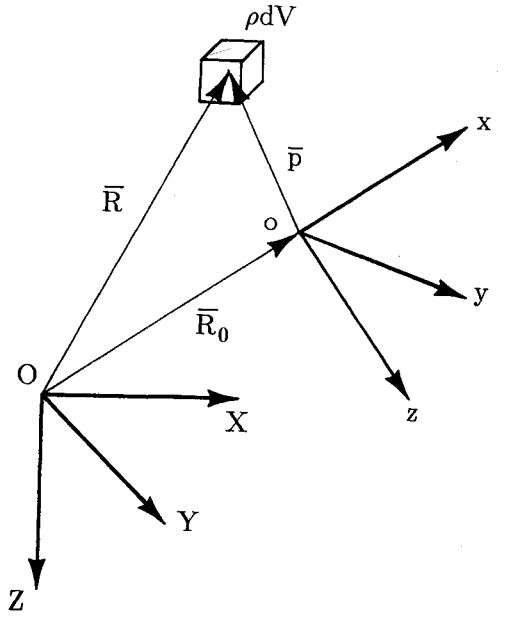

Fig. 1 Position of mass element.

ration, the change in the aerodynamic coefficients due to a small change in the configuration may be estimated from the closed-form expressions developed herein.

The modeling approach is applied to obtain a numerical model of an elastic airplane. As an example application of this approach, several quantitative models of a selected aircraft configuration are determined in which the frequencies of the vibration modes are varied parametrically to represent changes in structural stiffness. Linearized forms of these models are then evaluated to investigate the effects of the elastic degrees of freedom on the rigid-body-like dynamics.

Dynamics of Unconstrained Elastic Bodies—A Review

The inertial position (see Fig. 1) of a mass element ρdV of an elastic body can be written in terms of its position relative to a local reference system *oxyz* (with properties not yet specified), and the position of this local reference system relative to the inertial reference frame *OXYZ* (i.e., $\bar{R} = \bar{R}_0 + \bar{p}$). The kinetic energy of the body can then be written

$$T = \frac{1}{2}\int_V \frac{d\bar{R}}{dt} \cdot \frac{d\bar{R}}{dt} \rho \, dV \tag{1}$$

If the body-reference axes *oxyz* are rotating relative to inertial space with angular velocity $\bar{\omega}$, and if each mass element is treated as a point mass (Assumption 3), then

$$\frac{d\bar{R}}{dt} = \frac{d\bar{R}_0}{dt} + \frac{\delta\bar{p}}{\delta t} + \bar{\omega} \times \bar{p} \tag{2}$$

where $\delta/\delta t(\cdot)$ is the time derivative of $(\cdot)$ relative to the body-reference frame. The kinetic energy of the body then becomes

$$T = \frac{1}{2}\int_V \left\{ \frac{d\bar{R}_0}{dt} \cdot \frac{d\bar{R}_0}{dt} + 2\frac{d\bar{R}_0}{dt} \cdot \frac{\delta\bar{p}}{\delta t} + \frac{\delta\bar{p}}{\delta t} \cdot \frac{\delta\bar{p}}{\delta t} + 2\frac{\delta\bar{p}}{\delta t} \cdot (\bar{\omega} \times \bar{p}) + (\bar{\omega} \times \bar{p}) \cdot (\bar{\omega} \times \bar{p}) + 2(\bar{\omega} \times \bar{p}) \cdot \frac{d\bar{R}_0}{dt} \right\} \rho \, dV \tag{3}$$

The potential energy of the body consists of the elastic strain energy and the gravitational potential energy. The gravitational potential energy is simply

$$U_g = -\int_V \bar{g} \cdot (\bar{R}_0 + \bar{p}) \rho \, dV \tag{4}$$

where $\bar{g}$ is the gravitational acceleration vector. The elastic strain energy resulting from structural deformation is the work done on the structure in going from the undeformed reference shape to a deformed shape. If the position of a point of the body is represented by its undeformed position $\bar{s}(x,y,z)$ plus its deformation $\bar{d}(x,y,z,t)$ (i.e., $\bar{p} = \bar{s} + \bar{d}$ for each mass element), and D'Alembert's Principle is employed, then the strain energy can be written[5,6]

$$U_e = -\frac{1}{2}\int_V \frac{\delta^2\bar{d}}{\delta t^2} \cdot \bar{d} \rho \, dV \tag{5}$$

Mean Axes

In developing equations of motion of any unconstrained elastic system, inertial coupling can occur between the rigid-body degrees of freedom and the elastic degrees of freedom unless an appropriate choice for the local body-reference coordinate system is used. This noninertial reference system, which moves with the body but is not fixed to a material point in the body, is a "mean axis" system.[7,8]

The mean axes are defined such that the relative linear and angular momenta, due to elastic deformation, are zero at every instant. This implies that the mean axes must be chosen such that

$$\int_V \frac{\delta\bar{p}}{\delta t} \rho \, dV = \int_V \bar{p} \times \frac{\delta\bar{p}}{\delta t} \rho \, dV = 0 \tag{6}$$

These exact constraints are often difficult to apply directly, but "practical" constraints can be derived.

Recalling that the position of each mass element relative to the body-reference axes *oxyz* can be written

$$\bar{p} = \bar{s} + \bar{d} \tag{7}$$

and noting that the undeformed shape $\bar{s}$ is time invariant, Eq. (6) reduces to

$$\int_V \frac{\delta\bar{d}}{\delta t} \rho \, dV = \int_V (\bar{s} + \bar{d}) \times \frac{\delta\bar{d}}{\delta t} \rho \, dV = 0 \tag{8}$$

Now if the structural deformation is assumed to be small or the displacement and rate are colinear (Assumption 4), the cross product of the displacement $\bar{d}$ and the displacement rate $\delta\bar{d}/\delta t$ will be small, and to first-order accuracy can be neglected. If, in addition, the mass density of each element is constant (Assumption 5), Eq. (8) simplifies to

$$\frac{\delta}{\delta t}\int_V \bar{d} \rho \, dV = \frac{\delta}{\delta t}\int_V \bar{s} \times \bar{d} \rho \, dV = 0 \tag{9}$$

These are the "practical" mean axes constraints under the above assumptions.

Application of the mean axes constraints, Eq. (6), significantly simplifies the kinetic energy expression. Consider the second and fourth terms in Eq. (3). Using Eq. (6), they become

$$\int_V \frac{d\bar{R}_0}{dt} \cdot \frac{\delta\bar{p}}{\delta t} \rho \, dV = \frac{d\bar{R}_0}{dt} \cdot \int_V \frac{\delta\bar{p}}{\delta t} \rho \, dV \equiv 0 \tag{10}$$

and

$$\int_V \frac{\delta\bar{p}}{\delta t} \cdot (\bar{\omega} \times \bar{p}) \rho \, dV = \int_V \bar{p} \times \frac{\delta\bar{p}}{\delta t} \rho \, dV \cdot \bar{\omega} \equiv 0 \tag{11}$$

and as a result

$$T = \frac{1}{2}\int_V \left\{ \frac{d\bar{R}_0}{dt} \cdot \frac{d\bar{R}_0}{dt} + (\bar{\omega} \times \bar{p}) \cdot (\bar{\omega} \times \bar{p}) + \frac{\delta\bar{p}}{\delta t} \cdot \frac{\delta\bar{p}}{\delta t} + 2(\bar{\omega} \times \bar{p}) \cdot \frac{d\bar{R}_0}{dt} \right\} \rho \, dV \tag{12}$$

Locating the origin of the body-reference axes at the instantaneous center of mass of the body requires that

$$\bar{x}_{cm} = \int_V \bar{\rho}\,\rho\,dV \Big/ \int_V \rho\,dV = 0 \tag{13}$$

where $\bar{x}_{cm}$ is the position of the center of mass relative to the origin of the body-reference axes. This affects both the kinetic and potential energy expressions. The last term in the kinetic energy, Eq. (12), becomes zero since

$$\int_V (\bar{\omega} \times \bar{\rho}) \cdot \frac{d\bar{R}_0}{dt}\,\rho\,dV = \bar{\omega} \times \int_V \bar{\rho}\,\rho\,dV \cdot \frac{d\bar{R}_0}{dt} \equiv 0 \tag{14}$$

and so the kinetic energy becomes

$$T = \frac{1}{2}\int_V \left\{\frac{d\bar{R}_0}{dt} \cdot \frac{d\bar{R}_0}{dt} + (\bar{\omega} \times \bar{\rho}) \cdot (\bar{\omega} \times \bar{\rho}) + \frac{\delta\bar{\rho}}{\delta t} \cdot \frac{\delta\bar{\rho}}{\delta t}\right\} \rho\,dV \tag{15}$$

or, equivalently,

$$T = \frac{1}{2} M \frac{d\bar{R}_0}{dt} \cdot \frac{d\bar{R}_0}{dt} + \frac{1}{2}\bar{\omega}^T [I]\,\bar{\omega} + \frac{1}{2}\int_V \frac{\delta\bar{\rho}}{\delta t} \cdot \frac{\delta\bar{\rho}}{\delta t}\,\rho\,dV \tag{16}$$

where $[I]$ is the inertia tensor for the body and M is the mass of the body. Note that the inertia tensor is, in general, time varying due to elastic deformation. However, for small displacements, the inertia tensor is usually assumed to be constant (Assumption 6). Finally, the gravitational potential energy becomes

$$U_g = -\int_V (\bar{R}_0 + \bar{\rho}) \cdot \bar{g}\,\rho\,dV = -\bar{R}_0 \cdot \bar{g}\int_V \rho\,dV - \int_V \bar{\rho}\,\rho\,dV \cdot \bar{g} = -\bar{R}_0 \cdot g\mathrm{M} \tag{17}$$

Free Vibration Modes

The free vibration modes of an elastic body form a complete set of orthogonal functions that can be used to describe any forced motion of the body.[5,6] Further, the free vibration modes of an *unconstrained* elastic body can be used with the practical mean axes constraints to locate the origin, and determine the orientation of the body-reference axes that decouple the kinetic energy expression.

Assume that the free vibration modes of the body are available. Then, for that body undergoing general elastic deformation, the relative displacements can be described in terms of the mode shapes $\bar{\phi}_i(x,y,z)$ and generalized displacement coordinates $\eta_i(t)$, so

$$\bar{d} = \sum_{i=1}^{\infty} \bar{\phi}_i(x,y,z)\,\eta_i(t) \tag{18}$$

In terms of these quantities, the practical mean axes constraints can be written

$$\sum_{i=1}^{\infty} \frac{d\eta_i}{dt}\int_V \bar{\phi}_i\,\rho\,dV = \sum_{i=1}^{\infty} \frac{d\eta_i}{dt}\int_V \bar{s} \times \bar{\phi}_i\,\rho\,dV = 0 \tag{19}$$

These expressions then locate the mean body-reference axes, and can be interpreted as requiring the free vibration modes to be orthogonal to the rigid-body translational and rotational modes, respectively.

Applying Eq. (18) to the last term in the kinetic energy expression, Eq. (16), results in

$$\int_V \frac{\delta\bar{\rho}}{\delta t} \cdot \frac{\delta\bar{\rho}}{\delta t}\,\rho\,dV = \int_V \frac{\delta\bar{d}}{\delta t} \cdot \frac{\delta\bar{d}}{\delta t}\,\rho\,dV = \int_V \left\{\sum_{i=1}^{\infty} \bar{\phi}_i \frac{d\eta_i}{dt} \cdot \sum_{j=1}^{\infty} \bar{\phi}_j \frac{d\eta_j}{dt}\right\} \rho\,dV \tag{20}$$

This expression can be further simplified due to the orthogonality of the free vibration modes.[6,9] Since

$$\int_V \bar{\phi}_i \cdot \bar{\phi}_j\,\rho\,dV \equiv 0, \qquad i \neq j \tag{21}$$

then

$$\int_V \frac{\delta\bar{\rho}}{\delta t} \cdot \frac{\delta\bar{\rho}}{\delta t}\,\rho\,dV = \frac{1}{2}\sum_{i=1}^{\infty} M_i \dot{\eta}_i^2 \tag{22}$$

where the generalized mass of the ith mode is defined by

$$M_i = \int_V \bar{\phi}_i \cdot \bar{\phi}_i\,\rho\,dV \tag{23}$$

The kinetic energy equation now becomes

$$T = \frac{1}{2} M \frac{d\bar{R}_0}{dt} \cdot \frac{d\bar{R}_0}{dt} + \frac{1}{2}\bar{\omega}^T [I]\,\bar{\omega} + \frac{1}{2}\sum_{i=1}^{\infty} M_i \dot{\eta}_i^2 \tag{24}$$

Finally, the free-vibration modes can be used to express the strain energy.[2,9] Substituting Eq. (18) into Eq. (5) and noting that, for a given deformation, the strain energy of a body undergoing arbitrary forced motion is the same as for the body undergoing free vibration, results in

$$U_e = \frac{1}{2}\sum_{i=1}^{\infty} \omega_i^2 \eta_i^2 M_i \tag{25}$$

where ω_i is the in vacuo vibration frequency for the ith mode. The energy expressions for the unconstrained elastic body, Eqs. (17), (24), and (25), are now in a form that is conducive to the application of Lagrange's equation.

Elastic Airplane Equations of Motion

Recall that the desired equations of motion are to be expressed in terms of quantities defined in body-reference axes. However, application of Lagrange's equation requires the use of generalized coordinates describing motion relative to an inertial reference frame.

Consistent with these facts, define the *inertial* position of the origin of the body-reference (mean) axes (i.e., the instantaneous center of mass of the body) to be

$$\bar{R}_0 = x\hat{i} + y\hat{j} + z\hat{k} \tag{26}$$

where $\hat{i}$, $\hat{j}$, and $\hat{k}$ are unit vectors in each of the coordinate directions of the *body-reference axes*. Also, let

$$\frac{d\bar{R}_0}{dt} = \frac{\delta\bar{R}_0}{\delta t} + \bar{\omega} \times \bar{R}_0 \triangleq U\hat{i} + V\hat{j} + W\hat{k} \tag{27}$$

The usual Euler angles ϕ, θ, and ψ are used to define the inertial orientation of the body-reference axes, consistent with rigid aircraft analysis.[10] The vector defining the inertial angular velocity of the body-reference axis is

$$\bar{\omega} \triangleq p\hat{i} + q\hat{j} + r\hat{k} \tag{28}$$

where

$$p = \dot{\phi} - \dot{\psi}\sin\theta \tag{29a}$$

$$q = \dot{\psi}\cos\theta\sin\phi + \dot{\theta}\cos\phi \tag{29b}$$

$$r = \dot{\psi}\cos\theta\cos\phi - \dot{\theta}\sin\phi \tag{29c}$$

Then

$$U = \dot{x} + qz - ry, \qquad V = \dot{y} + rx - pz, \qquad W = \dot{z} + py - qx \tag{30}$$

Table 1 Elastic airplane equations of motion

$$M[\dot{U} - rV + qW + g\sin\theta] = Q_X$$

$$M[\dot{V} - pW + rU - g\sin\phi\cos\theta] = Q_Y$$

$$M[\dot{W} - qU + pV - g\cos\phi\cos\theta] = Q_Z$$

$$I_{xx}\dot{p} - (I_{xy}\dot{q} + I_{xz}\dot{r}) + (I_{zz} - I_{yy})qr + (I_{xy}r - I_{xz}q)p + (r^2 - q^2)I_{yz} + M[-g\cos\theta(y\cos\phi - z\sin\phi) + (\dot{W} + Vp - Uq)y - (\dot{V} + Ur - Wp)z] = Q_\phi$$

$$I_{yy}\dot{q} - (I_{xy}\dot{p} + I_{yz}\dot{r}) + (I_{xx} - I_{zz})pr + (I_{xy}p - I_{yx}r)q + (p^2 - r^2)I_{xz} + M[g(x\cos\theta\cos\phi + z\sin\theta) + (\dot{U} + qW - rV)z - (\dot{W} + pV - qU)x] = [Q_\phi\cos\phi\sin\theta - Q_\theta\sin\phi\cos\theta + Q_\psi\sin\phi]\sec\theta$$

$$I_{zz}\dot{r} - (I_{xz}\dot{p} + I_{yz}\dot{q}) + (I_{yy} - I_{xx})pq + (I_{xz}q - I_{yz}p)r + (q^2 - p^2)I_{xy} + M[-g(x\cos\theta\sin\phi + y\sin\theta) + (\dot{V} + Ur - Wp)x - (\dot{U} + qW - rV)y] = [Q_\phi\sin\phi\sin\theta + Q_\theta\cos\phi\cos\theta + Q_\psi\sin\phi]\sec\theta$$

$$\ddot{\eta}_i + \omega_i^2\eta_i = \frac{Q_{\eta_i}}{M_i} \qquad i = 1,2,3,\ldots$$

Now the kinetic and potential energies can be written as follows:

$$T = \frac{1}{2}M(U^2 + V^2 + W^2) + \frac{1}{2}[p\ q\ r][I]\begin{bmatrix} p \\ q \\ r \end{bmatrix} + \frac{1}{2}\sum_{i=1}^{\infty} M_i\dot{\eta}_i^2 \quad (31)$$

$$U_g = -Mg(-x\sin\theta + y\sin\phi\cos\theta + z\cos\phi\cos\theta) \quad (32)$$

$$U_e = \frac{1}{2}\sum_{i=1}^{\infty}\omega_i^2\eta_i^2 M_i \quad (33)$$

Substituting the expressions for U, V, and W, and p, q, and r [Eqs. (30) and (29) respectively] into Eq. (31) results in a kinetic energy expression in terms of the generalized coordinates (x,y,z,ϕ,θ,ψ, and η_i, $i = 1,2,\ldots$) and their rates. This allows direct application of Lagrange's equation

$$\frac{d}{dt}\left[\frac{\partial T}{\partial\dot{q}_i}\right] - \frac{\partial T}{\partial q_i} + \frac{\partial U}{\partial q_i} = Q_i \quad (34)$$

The equations that result may then be expressed in terms of U, V, W, p, q, and r via Eqs. (30) and (29). One form of these equations is given in Table 1. Notice that in deriving these equations it has been assumed that the inertia tensor is constant, in keeping with the small deformation assumption.

The Generalized Forces

The generalized forces may be determined from the Principle of Virtual Work[11]

$$Q_i = \frac{\partial}{\partial q_i}(\delta W) \quad (35)$$

where δW is the work associated with arbitrary virtual displacements of the generalized coordinates. Let the applied aerodynamic and propulsive forces and moments relative to *body-reference axes* be defined by

$$\bar{F} \triangleq X\hat{i} + Y\hat{j} + Z\hat{k}, \qquad \bar{M} \triangleq \underline{L}\hat{i} + \underline{M}\hat{j} + \underline{N}\hat{k} \quad (36)$$

where X, Y, and Z are simply the total aerodynamic and propulsive forces along each of the body-reference-axes directions, or

$$X = L\sin\alpha - D\cos\alpha\cos\beta + S\cos\alpha\sin\beta + T_x \quad (37a)$$

$$Y = -D\sin\beta - S\cos\beta + T_y \quad (37b)$$

$$Z = -L\cos\alpha - D\sin\alpha\cos\beta + S\sin\alpha\sin\beta + T_z \quad (37c)$$

L, D, and S are the lift, drag, and lateral aerodynamic forces on the aircraft in wind axes, α and β are the angle of attack and side slip angle, and T_x, T_y, and T_z are the components of the thrust force along the body-reference-axes directions. Similarly, $\underline{L}$, $\underline{M}$, and $\underline{N}$ are the total aerodynamic and propulsive moments about each of the body-reference-axes directions.

The moment about the origin of the *inertial axis* then is $\bar{M} + \bar{R}_0 \times \bar{F}$. Therefore, the virtual work, relative to the inertial reference frame, done by the aerodynamic and propulsive forces and moments is

$$\delta W = X\delta x + Y\delta y + Z\delta z + [\underline{L} + (yZ - zY)]\delta\phi_B + [\underline{M} + (zX - xZ)]\delta\theta_B + [\underline{N} + (xY - yX)]\delta\psi_B + \int_S \bar{P}(x,y,z)\cdot\sum_{i=1}^{\infty}\bar{\phi}_i\,\delta\eta_i\,dS \quad (38)$$

The displacements $\delta\phi_B$, $\delta\theta_B$, and $\delta\psi_B$ represent virtual rotations about each of the body-reference coordinate directions. They are related to virtual rotations of the generalized coordinates (ϕ, θ, and ψ) by the direction cosines relating the Euler-angle virtual rotations to the body-reference axes,[10,12] or

$$\delta\phi_B = \delta\phi - \delta\psi\sin\theta \quad (39a)$$

$$\delta\theta_B = \delta\theta\cos\phi + \delta\psi\cos\theta\sin\phi \quad (39b)$$

$$\delta\psi_B = -\delta\theta\sin\phi + \delta\psi\cos\theta\cos\phi \quad (39c)$$

The last term in Eq. (38) is the work done by the distributed surface pressures $\bar{P}(x,y,z)$, due to virtual displacements of each of the elastic generalized coordinates.

Applying Eq. (35) to the virtual work expression results in the completion of the equations of motion. However, it is noted that the three equations in Table 1 governing the rotational degrees of freedom can be simplified considerably since they explicitly contain the "translational" equations (from Table 1), and since $Q_X \equiv X$, $Q_Y \equiv Y$, and $Q_Z \equiv Z$. The simplified equations then become

$$I_{xx}\dot{p} - (I_{xy}\dot{q} + I_{xz}\dot{r}) + (I_{zz} - I_{yy})qr + (I_{xy}r - I_{xz}q)p + (r^2 - q^2)I_{yz} = Q_{\phi_B} \quad (40a)$$

$$I_{yy}\dot{q} - (I_{xy}\dot{p} + I_{yz}\dot{r}) + (I_{xx} - I_{zz})pr + (I_{yz}p - I_{xy}r)q + (p^2 - r^2)I_{xz} = Q_{\theta_B} \quad (40b)$$

$$I_{zz}\dot{r} - (I_{xz}\dot{p} + I_{yz}\dot{q}) + (I_{yy} - I_{xx})pq + (I_{xz}q - I_{yz}p)r + (q^2 - p^2)I_{xy} = Q_{\psi_B} \quad (40c)$$

where the generalized forces Q_{ϕ_B}, Q_{θ_B}, and Q_{ψ_B} are simply

$$Q_{\phi_B} = \underline{L}, \qquad Q_{\theta_B} = \underline{M}, \qquad Q_{\psi_B} = \underline{N} \quad (41)$$

The aerodynamic forces must now be determined. One way to accomplish this is by using aerodynamic strip theory.[4,13] The basic assumption of strip theory is that the aerodynamic lift (per unit span) l on a 2-D airfoil section is essentially dependent on the angle of attack of the section (α_s), or

$$l = \tfrac{1}{2}\rho V_0^2 c C_{l_\alpha}\alpha_s \quad (42)$$

where C_{l_α} is the lift curve slope and c is the chord of the airfoil,

and $\frac{1}{2}\rho V_0^2$ is the dynamic pressure. The lift on the airplane is then assumed to be expressed by

$$L = L_{\text{fuselage}} + \int_{-\frac{b}{2}}^{\frac{b}{2}} l_{\text{wing}}\,dy + \int_{-\frac{b_t}{2}}^{\frac{b_t}{2}} l_{\text{tail}}\,dy \tag{43}$$

To demonstrate the application of strip theory to elastic airplanes, and keeping the algebra simple, only a straight wing with span b will be considered here. Figure 2 depicts a section of wing and serves to define several important dimensions. Based on the geometry of the section and the contributions of vibration to the motion of the section about its elastic axis, the angle of attack of the section can be approximated by

$$\alpha_s = \alpha_v + i_s - q\left(\frac{\Delta x + e}{U}\right) + p\frac{y}{U} + \sum_{i=1}^{\infty}\left[\left(\frac{d\phi_i^b}{dx}\right)\eta_i + \frac{1}{U}\phi_i^b\dot{\eta}_i\right] \tag{44}$$

where $\alpha_v \triangleq \tan^{-1}[W/U]$ is the angle of attack of the vehicle (i.e., of the body-reference axes), i_s is the structural incidence of the section, ϕ_i^b is the wing-bending (z) displacement due to the ith mode, and $d\phi_i^b/dx$ is the effective torsional displacement of the section due to the ith mode, assuming no changes in section camber.

Substituting the above expression for the section angle of attack, Eq. (43) results in an expression for the lift of the entire wing:

$$L_w = \frac{\rho V_0^2 S}{2}\left[C_{L_0} + C_{L_\alpha}\alpha_v + C_{L_p}p + C_{L_q}q + + C_{L_\delta}\delta + \sum_{i=1}^{\infty}\left(C_{L_{\eta_i}}\eta_i + C_{L_{\dot{\eta}_i}}\dot{\eta}_i\right)\right] \tag{45}$$

where the definitions of the effective force coefficients are given in Table 2. The effect of control surface deflection δ has been accounted for by introducing the control effectiveness C_{L_δ}. Notice that although these coefficients are not all nondimensional, they can easily be redefined to be nondimensional and consistent with standard practice.[12] Also, since this example only considers a straight wing, lag-due-to-downwash effects are not included and there are no $\dot{\alpha}$ coefficients that are common in rigid-body aerodynamics. However, there are no problems associated with adding such terms using standard techniques.[10,12]

Similar expressions can be obtained for the moments associated with the span wise distribution of lift. The pitching moment about the origin of the body-reference axes (i.e., the center of mass) can be expressed as follows:

$$M = \frac{\rho V_0^2 S\bar{c}}{2}\left[C_{M_0} + C_{M_\alpha}\alpha_v + C_{M_p}p + C_{M_q}q + C_{M_\delta}\delta + \sum_{i=1}^{\infty}\left(C_{M_{\eta_i}}\eta_i + C_{M_{\dot{\eta}_i}}\dot{\eta}_i\right)\right] \tag{46}$$

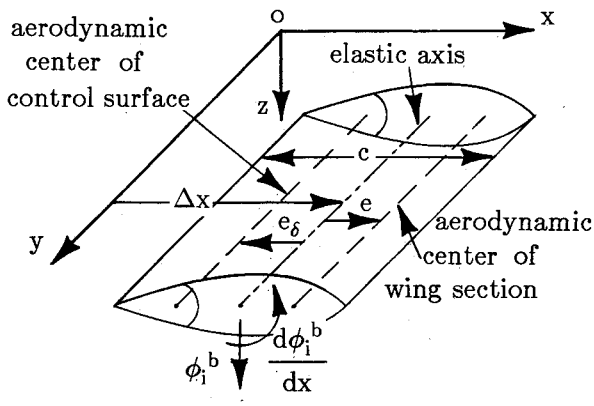

Fig. 2 Wing section and dimensions.

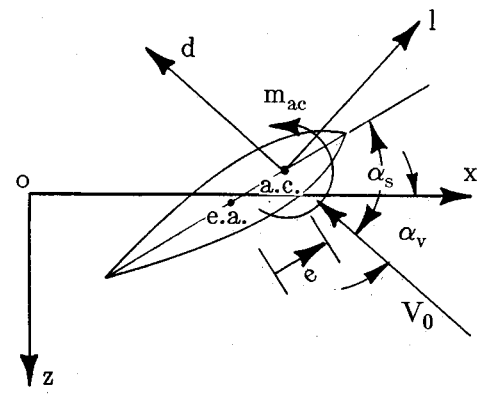

Fig. 3 Typical 2-D section.

Table 2 Effective lift, pitching moment, and generalized force coefficients

Coefficient	Definition	Coefficient	Definition	Coefficient	Definition
C_{L_0}	$\frac{1}{S}\int_{-\frac{b}{2}}^{\frac{b}{2}}(C_{l_0}+C_{l_\alpha}i_s)\,c\,dy$	C_{M_0}	$\frac{1}{S\bar{c}}\int_{-\frac{b}{2}}^{\frac{b}{2}}\left[C_{\text{mac}}+(C_{l_0}+C_{l_\alpha}i_s)\left(\frac{\Delta x+e}{c}\right)\right]c^2\,dy$	$C_0^{A_i}$	$-\frac{1}{S\bar{c}}\int_{-\frac{b}{2}}^{\frac{b}{2}}(C_{l_0}+C_{l_\alpha}i_s)\phi_i^b c\,dy$
C_{L_α}	$\frac{1}{S}\int_{-\frac{b}{2}}^{\frac{b}{2}}C_{l_\alpha}c\,dy$	C_{M_α}	$\frac{1}{S\bar{c}}\int_{-\frac{b}{2}}^{\frac{b}{2}}C_{l_\alpha}\left(\frac{\Delta x+e}{c}\right)c^2\,dy$	$C_\alpha^{A_i}$	$-\frac{1}{S\bar{c}}\int_{-\frac{b}{2}}^{\frac{b}{2}}C_{l_\alpha}\phi_i^b c\,dy$
C_{L_p}	$\frac{1}{S}\int_{-\frac{b}{2}}^{\frac{b}{2}}C_{l_\alpha}\frac{y}{U}c\,dy$	C_{M_p}	$\frac{1}{S\bar{c}}\int_{-\frac{b}{2}}^{\frac{b}{2}}C_{l_\alpha}\frac{y(\Delta x+e)}{Uc}c^2\,dy$	$C_p^{A_i}$	$-\frac{1}{S\bar{c}}\int_{-\frac{b}{2}}^{\frac{b}{2}}C_{l_\alpha}\frac{y}{U}\phi_i^b c\,dy$
C_{L_q}	$\frac{1}{S}\int_{-\frac{b}{2}}^{\frac{b}{2}}C_{l_\alpha}\left(\frac{\Delta x+e}{U}\right)c\,dy$	C_{M_q}	$\frac{1}{S\bar{c}}\int_{-\frac{b}{2}}^{\frac{b}{2}}C_{l_\alpha}\frac{(\Delta x+e)^2}{Uc}c^2\,dy$	$C_q^{A_i}$	$\frac{1}{S\bar{c}}\int_{-\frac{b}{2}}^{\frac{b}{2}}C_{l_\alpha}\left(\frac{\Delta x+e}{U}\right)\phi_i^b c\,dy$
C_{L_δ}	$\frac{1}{S}\int_{-\frac{b}{2}}^{\frac{b}{2}}C_{l_\delta}c\,dy$	C_{M_δ}	$\frac{1}{S\bar{c}}\int_{-\frac{b}{2}}^{\frac{b}{2}}C_{l_\delta}\left(\frac{\Delta x-e_\delta}{c}\right)c^2\,dy$	$C_\delta^{A_i}$	$-\frac{1}{S\bar{c}}\int_{-\frac{b}{2}}^{\frac{b}{2}}C_{l_\delta}\phi_i^b c\,dy$
$C_{L_{\eta_i}}$	$\frac{1}{S}\int_{-\frac{b}{2}}^{\frac{b}{2}}C_{l_\alpha}\left(\frac{d\phi_i^b}{dx}\right)c\,dy$	$C_{M_{\eta_i}}$	$\frac{1}{S\bar{c}}\int_{-\frac{b}{2}}^{\frac{b}{2}}C_{l_\alpha}\left(\frac{\Delta x+e}{c}\right)\left(\frac{d\phi_i^b}{dx}\right)c^2\,dy$	$C_{\eta_j}^{A_i}$	$-\frac{1}{S\bar{c}}\int_{-\frac{b}{2}}^{\frac{b}{2}}C_{l_\alpha}\left(\frac{d\phi_i^b}{dx}\right)\phi_j^b c\,dy$
$C_{L_{\dot{\eta}_i}}$	$\frac{1}{S}\int_{-\frac{b}{2}}^{\frac{b}{2}}C_{l_\alpha}\frac{1}{U}\phi_i^b c\,dy$	$C_{M_{\dot{\eta}_i}}$	$\frac{1}{S\bar{c}}\int_{-\frac{b}{2}}^{\frac{b}{2}}C_{l_\alpha}\left(\frac{\Delta x+e}{Uc}\right)\phi_i^b c^2\,dy$	$C_{\eta_j}^{A_i}$	$-\frac{1}{S\bar{c}}\int_{-\frac{b}{2}}^{\frac{b}{2}}C_{l_\alpha}\frac{1}{U}\phi_i^b\phi_j^b c\,dy$

Table 3 Example elastic airplane generalized forces

$$Q_X = \frac{\rho V_0^2 S}{2}\left(C_{X_0} + C_{X_\alpha}\alpha + C_{X_\delta}\delta + \sum_{i=1}^{\infty} C_{X_{\eta_i}}\eta_i\right) + \frac{\rho V_0 S\bar{c}}{4}\left(C_{X_{\dot\alpha}}\dot\alpha + C_{X_q}q + \sum_{i=1}^{\infty} C_{X_{\dot\eta_i}}\dot\eta_i\right) + T_X$$

$$Q_Y = \frac{\rho V_0^2 S}{2}\left(C_{Y_0} + C_{Y_\beta}\beta + C_{Y_\delta}\delta + \sum_{i=1}^{\infty} C_{Y_{\eta_i}}\eta_i\right) + \frac{\rho V_0 Sb}{4}\sum_{i=1}^{\infty} C_{Y_{\dot\eta_i}}\dot\eta_i + T_y$$

$$Q_Z = \frac{\rho V_0^2 S}{2}\left(C_{Z_0} + C_{Z_\alpha}\alpha + C_{Z_\delta}\delta + \sum_{i=1}^{\infty} C_{Z_{\eta_i}}\eta_i\right) + \frac{\rho V_0 S\bar{c}}{4}\left(C_{Z_{\dot\alpha}}\dot\alpha + C_{Z_p}p + C_{Z_q}q + \sum_{i=1}^{\infty} C_{Z_{\dot\eta_i}}\dot\eta_i\right) + T_z$$

$$Q_{\phi_B} = \frac{\rho V_0^2 Sb}{2}\left(C_{L_0} + C_{L_\beta}\beta + C_{L_\delta}\delta + \sum_{i=1}^{\infty} C_{L_{\eta_i}}\eta_i\right) + \frac{\rho V_0 Sb^2}{4}\left(C_{L_p}p + C_{L_r}r + \sum_{i=1}^{\infty} C_{L_{\dot\eta_i}}\dot\eta_i\right) + L_T$$

$$Q_{\theta_B} = \frac{\rho V_0^2 S\bar{c}}{2}\left(C_{M_0} + C_{M_\alpha}\alpha + C_{M_\delta}\delta + \sum_{i=1}^{\infty} C_{M_{\eta_i}}\eta_i\right) + \frac{\rho V_0 S\bar{c}^2}{4}\left(C_{M_{\dot\alpha}}\dot\alpha + C_{M_q}q + \sum_{i=1}^{\infty} C_{M_{\dot\eta_i}}\dot\eta_i\right) + M_T$$

$$Q_{\psi_B} = \frac{\rho V_0^2 Sb}{2}\left(C_{N_0} + C_{N_\beta}\beta + C_{N_\delta}\delta + \sum_{i=1}^{\infty} C_{N_{\eta_i}}\eta_i\right) + \frac{\rho V_0 Sb^2}{4}\left(C_{N_p}p + C_{N_r}r + \sum_{i=1}^{\infty} C_{N_{\dot\eta_i}}\dot\eta_i\right) + N_T$$

$$Q_{\eta_j} = \frac{\rho V_0^2 S\bar{c}}{2}\left(C_0^{\eta_j} + C_\alpha^{\eta_j}\alpha + C_\beta^{\eta_j}\beta + C_\delta^{\eta_j}\delta + \sum_{i=1}^{\infty} C_{\eta_i}^{\eta_j}\eta_i\right) + \frac{\rho V_0 S\bar{c}^2}{4}\left(C_{\dot\alpha}^{\eta_j}\dot\alpha + C_p^{\eta_j}p + C_q^{\eta_j}q + C_r^{\eta_j}r + \sum_{i=1}^{\infty} C_{\dot\eta_i}^{\eta_j}\dot\eta_i\right)$$

The definitions for these coefficients, ignoring section drag effects, are given in Table 2. Expressions for the other forces and moments and their corresponding coefficients can be determined in a manner similar to those above.

The determination of the generalized force expressions for the elastic degrees of freedom (i.e., Q_{η_i}, $i = 1,2,...$) follows a similar development. Figure 3 depicts the forces and moments (per unit span) that act on a typical wing section. The two degrees of freedom due to elastic deflection of the section, again assuming no change in camber, are plunge and twist. As a result, the work due to the elastic deflection of the section can be written as the sum of two terms, one associated with bending and the other with torsion, again ignoring section drag effects.

$$W_{\text{bend}} = -l\cos\alpha_v \sum_{i=1}^{\infty} \phi_i^b \eta_i \tag{47}$$

$$W_{\text{torsion}} = (m_{ac} + l\,e\cos\alpha_s)\sum_{i=1}^{\infty}\left(\frac{\mathrm{d}\phi_i^b}{\mathrm{d}x}\right)\eta_i \tag{48}$$

From these work expressions, the generalized forces for the structural degrees of freedom can be determined to be

$$Q_{\eta_i} = \int_{-\frac{b}{2}}^{\frac{b}{2}}\left\{(-l\cos\alpha_v\phi_i^b) + \left[(m_{ac} + l\,e\cos\alpha_s)\left(\frac{\mathrm{d}\phi_i^b}{\mathrm{d}x}\right)\right]\right\}\mathrm{d}y \tag{49}$$

Assuming $\cos\alpha_s \approx \cos\alpha_v$, then the above generalized force can be approximated as

$$Q_{\eta_i} \approx (A_i + B_i)\cos\alpha_v + C_i \tag{50}$$

where

$$A_i = -\int_{-\frac{b}{2}}^{\frac{b}{2}} l\,\phi_i^b\,\mathrm{d}y \qquad B_i = -\int_{-\frac{b}{2}}^{\frac{b}{2}} l\,e\left(\frac{\mathrm{d}\phi_i^b}{\mathrm{d}x}\right)\mathrm{d}y$$

$$C_i = -\int_{-\frac{b}{2}}^{\frac{b}{2}} m_{ac}\left(\frac{\mathrm{d}\phi_i^b}{\mathrm{d}x}\right)\mathrm{d}y \tag{51}$$

Generalized force coefficients for the elastic degrees of freedom (e.g., $C_{(\cdot)}^{A_i}$) can now be defined analogously to the conventional aerodynamic force coefficients. For example, one can express

$$A_i = \frac{\rho V_0^2 S\bar{c}}{2}\left[C_0^{A_i} + C_\alpha^{A_i}\alpha_v + C_p^{A_i}p + C_q^{A_i}q + C_\delta^{A_i}\delta + \sum_{j=1}^{\infty}(C_{\eta_j}^{A_i}\eta_i + C_{\dot\eta_j}^{A_i}\dot\eta_j)\right] \tag{52}$$

where the definitions for the coefficients are given in Table 2. Coefficients in the generalized force terms B_i and C_i are expressed in a similar manner.

By combining all the coefficients for a particular generalized force Q, one can obtain total force coefficients. For example, consider Q_{η_i}, expanded in terms of the force coefficients, or

$$Q_{\eta_i} = \frac{\rho V_0^2 S\bar{c}}{2}\left\{\left[(C_0^{A_i} + C_0^{B_i}) + (C_\alpha^{A_i} + C_\alpha^{B_i})\alpha_v + (C_p^{A_i} + C_p^{B_i})p + (C_q^{A_i} + C_q^{B_i})q + (C_\delta^{A_i} + C_\delta^{B_i})\delta + \sum_{j=1}^{\infty}(C_{\eta_j}^{A_i} + C_{\eta_j}^{B_i})\eta_j + \sum_{j=1}^{\infty}(C_{\dot\eta_j}^{A_i} + C_{\dot\eta_j}^{B_i})\dot\eta_j\right]\cos\alpha_v + \left[C_0^{C_i} + C_\alpha^{C_i}\alpha_v + C_p^{C_i}p + C_q^{C_i}q + C_\delta^{C_i}\delta + \sum_{j=1}^{\infty}(C_{\eta_j}^{C_i}\eta_j + C_{\dot\eta_j}^{C_i}\dot\eta_j)\right]\right\} \tag{53}$$

By grouping like terms this generalized force can be expressed as

$$Q_{\eta_i} = \frac{\rho V_0^2 S\bar{c}}{2}\left(C_0^{\eta_i} + C_\alpha^{\eta_i}\alpha_v + C_\delta^{\eta_i}\delta + \sum_{j=1}^{\infty} C_{\eta_j}^{\eta_i}\eta_j\right) + \frac{\rho V_0 S\bar{c}^2}{4}\left(C_p^{\eta_i}p + C_q^{\eta_i}q + \sum_{j=1}^{\infty} C_{\dot\eta_j}^{\eta_i}\dot\eta_j\right) \tag{54}$$

where the definitions of the nondimensional total force coefficients are obvious.

The nonlinear generalized force expressions can now be written in terms of these total force coefficients. The result is a set of generalized force expressions similar to those given in Table 3. The equations of motion then consist of the combination of the equations in Table 1, Table 3, and Eq. (40).

Numerical Results

The study vehicle is a large elastic airplane similar to that depicted in Fig. 4. The geometry, mass, and inertia properties of this airplane are summarized in Table 4. The numerical model will be generated for the longitudinal axis only, using four structural modes. The shapes of these modes are depicted in Fig. 5.

The nonlinear numerical model was linearized about the following flight condition: straight and level cruise at an altitude of 5000 ft and at a Mach number of 0.6. The force coefficients of the airplane at this flight condition, analogous to those in Table 3, are summarized in Table 5, along with the dimensions of the quantities of interest. The in vacuo vibration frequencies of the structural modes are varied in the model to

represent varying levels of structural flexibility and each mode has an equivalent modal damping of 0.02. Table 6 defines the vibration frequencies used in this example for two flexible configurations. Configuration C1 represents a rigid aircraft, configuration C2 corresponds to a baseline flexible vehicle, and configuration C3 represents a more flexible vehicle. The rigid-body model is obtained, of course, by ignoring all the effects of flexibility, i.e., all the η_i's are assumed to be zero.

The input and response of interest in this example are elevator deflection, δ (in deg), and pitch rate q measured at the cockpit (in rad/s). The poles, zeros, and transfer-function gains for the $q(s)/\delta(s)$ transfer functions of the three configurations are given in Table 7, and the frequency responses are shown in Figs. 6 and 7.

If a lower-order $q(s)/\delta(s)$ transfer function of the elastic aircraft is desired, several model reduction methods can be used, modal truncation or modal residualization, for example. If the full-order transfer function in partial fraction form (i.e., poles and impulse residues) is

$$G(s) = \sum_{i=1}^{n} \frac{R_i}{s + p_i} \tag{55}$$

then the truncated-mode model is

$$G_T(s) = \sum_{i=1}^{m} \frac{R_i}{s + p_i} \tag{56}$$

where $m < n$.

Table 4 Geometry, mass, and inertia of study vehicle

Geometry	$\bar{c} = 15.3$ ft (mean chord) $b = 70.0$ ft (wing span) $S = 1946$ ft^2 (planform area) $\Lambda = 65$ deg (sweep angle)
Weight	$W = 288{,}017$ lb (net weight)
Inertia	$I_{xx} = 950{,}000$ slug-ft^2 $I_{yy} = 6{,}400{,}000$ slug-ft^2 $I_{zz} = 7{,}100{,}000$ slug-ft^2 $I_{xz} = -52{,}700$ slug-ft^2 $I_{xy} = I_{yz} = 0$
Modal generalized masses[a]	$M_1 = 183.6$ slug-ft^2 $M_2 = 9586.5$ slug-ft^2 $M_3 = 1334.4$ slug-ft^2 $M_4 = 43{,}596.9$ slug-ft^2

[a]Modal damping, $T_i = 0.02$, $i = 1,2,3,4$

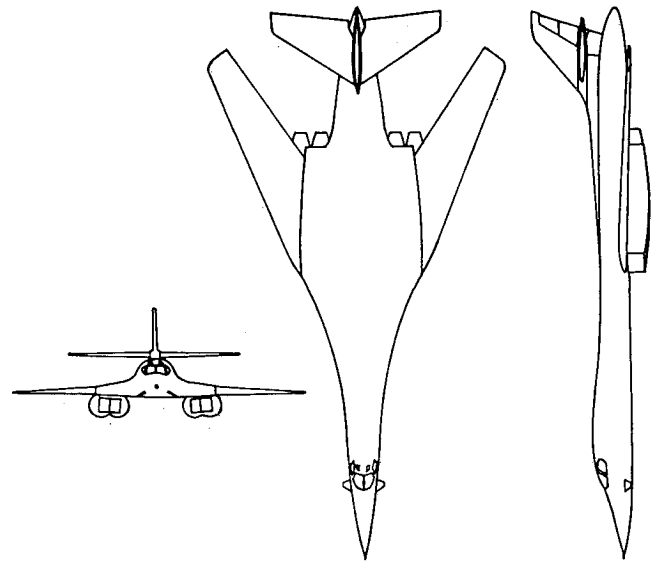

Fig. 4 Geometry of study vehicle.

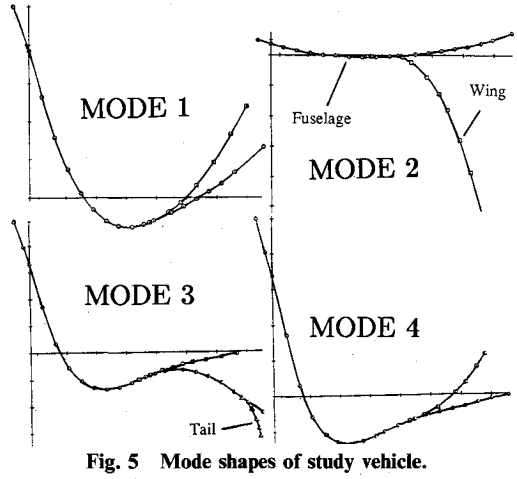

Fig. 5 Mode shapes of study vehicle.

Table 6 Vehicle configurations

	In vacuo modal vibration frequencies (rad/s)			
Configuration	Mode 1	Mode 2	Mode 3	Mode 4
C1 (rigid)	—	—	—	—
C2 (baseline)	12.57	14.07	21.17	22.05
C3	6.29	7.04	10.59	11.03

Table 5 Total force coefficients for baseline study vehicle

							$i =$			
Q_X		Q_Z		Q_{θ_B}		$Q_\eta i$	1	2	3	4
C_{X_0}	−0.028	C_{Z_0}	−0.34	C_{M_0}	−0.252	$C_0^{\eta i}$	0.0	0.0	0.0	0.0
C_{X_α}	0.0035	C_{Z_α}	−0.051	C_{M_α}	−0.029	$C_\alpha^{\eta i}$	−2.6e-04	4.5e-04	2.6e-04	5.84e-07
$C_{X_{\dot\alpha}}$	0.0	$C_{Z_{\dot\alpha}}$	0.0	$C_{M_{\dot\alpha}}$	−4.3	$C_{\dot\alpha}^{\eta i}$	0.0	0.0	0.0	0.0
C_{X_q}	−1.7	C_{Z_q}	14.7	C_{M_q}	−34.75	$C_q^{\eta i}$	−9.49e-02	1.16e-02	3.97e-02	2.83e-05
C_{X_δ}	0.00267	C_{Z_δ}	−0.0076	C_{M_δ}	−0.045	$C_\delta^{\eta i}$	−2.24e-04	−1.12e-03	4.46e-04	2.56e-06
$C_{X_{\eta_1}}$	0.0	$C_{Z_{\eta_1}}$	−0.0288	$C_{M_{\eta_1}}$	−0.0321	$C_{\eta_1}^{\eta i}$	5.85e-05	4.21e-03	2.91e-04	2.21e-05
$C_{X_{\eta_2}}$	0.0	$C_{Z_{\eta_2}}$	0.306	$C_{M_{\eta_2}}$	−0.025	$C_{\eta_2}^{\eta i}$	−9.0e-05	−9.22e-02	1.44e-03	−1.32e-04
$C_{X_{\eta_3}}$	0.0	$C_{Z_{\eta_3}}$	0.0148	$C_{M_{\eta_3}}$	0.0414	$C_{\eta_3}^{\eta i}$	3.55e-04	1.97e-03	−3.46e-04	9.68e-06
$C_{X_{\eta_4}}$	0.0	$C_{Z_{\eta_4}}$	−0.0140	$C_{M_{\eta_4}}$	−0.0183	$C_{\eta_4}^{\eta i}$	1.20e-04	3.37e-03	1.44e-04	1.77e-03
$C_{X_{\dot\eta_1}}$	0.0	$C_{Z_{\dot\eta_1}}$	−0.0848	$C_{M_{\dot\eta_1}}$	−0.159	$C_{\dot\eta_1}^{\eta i}$	−4.20e-04	8.71e-03	−6.29e-04	−5.55e-05
$C_{X_{\dot\eta_2}}$	0.0	$C_{Z_{\dot\eta_2}}$	1.03	$C_{M_{\dot\eta_2}}$	1.23	$C_{\dot\eta_2}^{\eta i}$	−1.97e-04	−2.98e-01	1.95e-02	4.09e-04
$C_{X_{\dot\eta_3}}$	0.0	$C_{Z_{\dot\eta_3}}$	0.0608	$C_{M_{\dot\eta_3}}$	0.172	$C_{\dot\eta_3}^{\eta i}$	6.50e-04	4.19e-03	−8.77e-06	−4.66e-05
$C_{X_{\dot\eta_4}}$	0.0	$C_{Z_{\dot\eta_4}}$	−0.0199	$C_{M_{\dot\eta_4}}$	−0.0496	$C_{\dot\eta_4}^{\eta i}$	−1.40e-04	4.15e-03	−1.31e-03	7.99e-02

Note α and δ in deg q and $\dot\alpha$ in rad/s, η_i in rad, and $\dot\eta_i$ in rad/s.

Table 7 $q(s)/\delta(s)$ transfer-function data

Configuration							
C1	C2	C2	C2	C3	C3	C3	
Rigid	Full order	Residualized	Truncated	Full order	Residualized	Truncated	
T.F. gain	−0.0929	−0.417	0.0045	−0.0100	−0.417	0.0045	−0.0100
Zeros	0.0 −0.0161 −0.386	0.0 −0.0143 −0.400 [0.0423,4.883] [0.147,17.79] [0.0136,22.04] [0.0125,23.59]	0.0 −0.0134 −0.449 42.36	[0.290,0.0213] −0.519	0.0 −0.0036 −0.7183 [0.0044,1.414] [0.0072,11.01] [−0.0117,11.87] [0.206,13.02]	0.0 −0.0037 −1.541 2.754	[0.290,0.021] −0.519
Poles	[0.0929,0.059] [0.356,1.97]	[0.0951,0.0551] [0.358,1.830] [0.0374,12.40] [0.149,18.03] [0.021,21.25] [0.0136,22.04]	[0.0951,0.0551] [0.358,1.830]	[0.0951,0.0551] [0.358,1.830]	0.0007 −0.0083 [0.413,1.255] [0.0736,6.02] [0.021,10.78] [0.007,11.01] [0.194,13.30]	0.0007 −0.0083 [0.413,1.255]	0.0007 −0.0083 [0.413,1.255]

Note: Complex conjugate poles and zeros are written [ζ, ω (rad/s)].

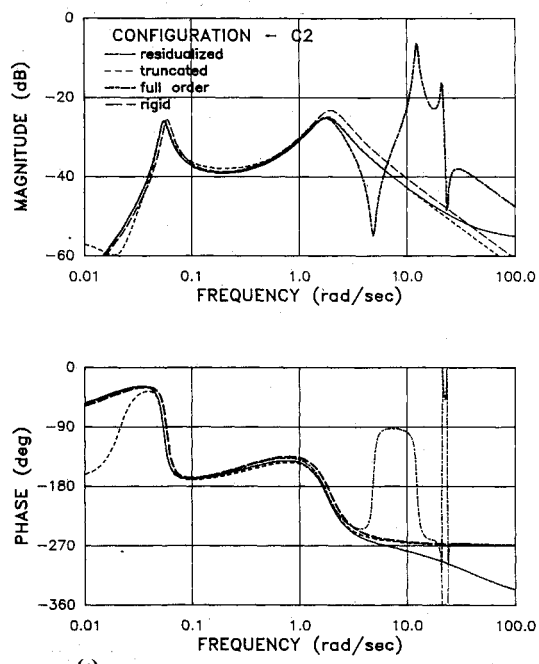

Fig. 6 $\frac{q(s)}{\delta(s)}$ frequency response comparison: Configuration 2.

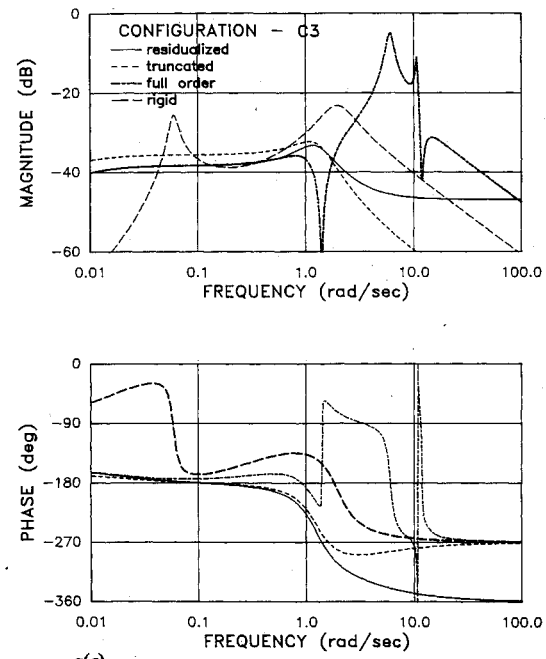

Fig. 7 $\frac{q(s)}{\delta(s)}$ frequency response comparison: Configuration 3.

Similarly, the residualized-mode model is

$$G_R(s) = \sum_{i=1}^{m} \frac{R_i}{s + p_i} + \sum_{i=m+1}^{n} \frac{R_i}{p_i} \tag{57}$$

Truncating all four aeroelastic modes, for example, results in lower-order transfer functions with poles identical to a subset of the poles in the full-order model, and the transfer-function gains and zeros depend on the values of the impulse residues R_i of the retained modes. Residualizing the same aeroelastic modes also results in lower-order transfer functions with the same poles that are a subset of the poles of the full-order transfer function, but with transfer-function gains and zeros that depend on the values of *all* of the residues and on the poles of the *deleted* modes.

For this example, let the desired order of the transfer functions be that of the rigid model. The resulting reduced-order transfer functions for the flexible configurations are presented in Table 7 along with the rigid-model transfer functions. The rigid-model transfer function and the reduced-order flexible models (i.e., truncated and residualized) are all fourth order, while the full-order model is, of course, twelfth order.

Figure 6 shows the frequency responses of the rigid model, the two reduced-order models, and the full-order model for the baseline configuration (C2). Figure 7 shows the same set of frequency responses, but for the more flexible configuration (C3). Review of these results reveal that the residualized model is the better reduced-order approximation for these flexible aircraft dynamics. The frequency response of the baseline configuration indicates a good match up to about 2 rad/s. However, as flexibility increases (e.g., configuration C3), even the residualized model demonstrates significant errors. Though the magnitude is well approximated to about 1 rad/s, the phase error is significant beyond 0.1 rad/s.

The potential problems associated with reducing the order of the aircraft model before the important dynamics are identified are clear from these results. Configuration C3 has an unstable phugoid mode, also reflected in its reduced-order models. But the rigid model has a stable phugoid mode. In addition, had the surge degree of freedom been neglected in the modeling process from the outset (i.e., short period approximation), the instability would not have been predicted, regardless of whether flexibility was included in the model or not.

Finally, notice that the rigid model differs significantly from the flexible model in both configurations. But the more flexible configuration has a drastically different frequency response from the rigid model over the entire frequency range, underscoring the significance of the aeroelastic effects.

Summary and Conclusion

The development of an integrated model for aeroelastic aircraft has been presented. The equations of motion were obtained from first principles (i.e., Lagrange's equation and the principle of Virtual Work) and the simplifying assumptions were stated. Expressions for the generalized aerodynamic forces were determined from strip theory and expressed as closed-form integral equations. The resulting equations of motion are in a form that is a direct extension of that for a rigid vehicle.

Since the equations for the generalized forces are in closed form, the effect of various parameters can be observed and insight into the effects of parameter variation can more readily be obtained. This approach can also be used to obtain a model very early in the design process, which may be useful for exploring the potential effects of aeroelasticity on the vehicle dynamics and flight-control synthesis.

Not only the modeling approach, but model simplification can lead to significant variations in the vehicle model. As shown in the numerical example, the residualized-mode models, obtained from the "full" aeroelastic models, can account for the static effects of elastic coupling in the rigid-body degrees of freedom, and better approximate the dynamics of a moderately flexible vehicle. However, as flexibility increases, even a residualized-mode model can lead to significant errors. Finally, a model obtained under a rigid-body assumption may not be very accurate, even when the form of the desired model is that of a rigid vehicle.

Acknowledgments

This research was supported by NASA Langley Research Center under Grant NAG-1-254. Mr. William Grantham and Mr. Jerry Elliott have served as technical monitors. This support is appreciated.

References

[1]Gilbert, M. G., Schmit, D. K., and Weisshaar, T. A., "Quadratic Synthesis of Integrated Active Control for an Aeroelastic Forward-Swept-Wing Aircraft," *Journal of Guidance, Control, and Dynamics*, Vol. 7, March–April 1984, pp. 190–196.

[2]Bisplinghoff, R. L. and Ashley, H., *Principles of Aeroelasticity*, Wiley, New York, 1962.

[3]Schwanz, R. C., Cerra, J. J., and Blair M., "Dynamic Modeling Uncertainty Affecting Control System Design," AIAA Paper 84-1057, May 1984.

[4]Yates, E. C., "Calculation of Flutter Characteristics ... By a Modified Strip Analysis," NACA RM L57L10, March 1958.

[5]Sokolnikoff, I. S., *Mathematical Theory of Elasticity*, McGraw-Hill, New York, 1956.

[6]Soedel, W., *Vibrations of Shells and Plates*, Dekker, Inc., New York, 1981.

[7]Milne, R. D., "Some Remarks on the Dynamics of Deformable Bodies," *AIAA Journal*, Vol. 6, March 1968, p. 556.

[8]Milne, R. D., "Dynamics of the Deformable Aeroplane, Parts I and II," Her Majesty's Stationery Office, Reports and Memoranda No. 3345, Sept. 1962.

[9]Hurty, W. C. and Rubinstein, M. F., *Dynamics of Structures*, Prentice-Hall, Inc., New York, 1964.

[10]Roskam, J., *Airplane Flight Dynamics and Automatic Flight Controls—Part I*, Roskam Aviation and Engineering Corp., Ottawa, KS, 1982.

[11]Synge, S. L. and Griffith, B. A., *Principles of Mechanics*, McGraw-Hill, New York, 1959.

[12]Etkin, B., *Dynamics of Flight—Stability and Control*, Wiley, New York, 1982.

[13]Gilbert, M. G., "Dynamic Modeling and Active Control of Aeroelastic Aircraft," Masters Thesis, Purdue Univ., West Lafayette, IN, Dec. 1982.